Modeling of Stacked Single-Layer Coils Wound with Bi2223 Tapes Using a Lumped Constant Circuit*)

Tetsuhiro OBANA and Nozomu NANATO[1)]

National Institute for Fusion Science, Toki 509-5292, Japan
[1)]*Okayama University of Science, Okayama 700-0005, Japan*

(Received 12 November 2020 / Accepted 20 February 2021)

Stacked single-layer (SSL) coils wound with Bi2223 HTS tapes were modeled with a lumped circuit. Using the model, we investigated the effect of the joint resistance at coil terminals on the generated voltage for the SSL coils. The investigation shows that the joint resistance must be reduced as much as possible to restrain the voltage occurred in the SSL coils and each joint resistance should be uniform to make the current distribution uniform in the SSL coils. Additionally, we investigated the effect of inductance on the current distribution in the SSL coils and the effect of the tape's degradation on the coil performance. As a result, the current distribution of the SSL coils can be uniform due to the joint resistance even though the SSL coils have different inductances in each coil winding. Further, the current distribution and the voltage of the SSL coils are influenced by the tape's degradation.

Keywords: HTS coil, Bi2223 tape, stacked single-layer (SSL) coil, current distribution, modeling

DOI: 10.1585/pfr.16.2405051

1. Introduction

To conduct a large current energization test of superconductors used for fusion magnets, we have been developing a compact and lightweight power source with the large current [1, 2]. The power source is composed of a transformer using high temperature superconducting (HTS) coils. In the transformer, the primary coil and the secondary coil are wound with Bi2223 tapes, and the height of both coils are the same. Regarding the coil configuration, the primary coil is composed of two coil windings the diameters of which are different. And the secondary coil is composed of single-layer coil windings which are stacked vertically. To reduce the leakage inductance of the transformer as much as possible, the secondary coil is sandwiched with the primary coil. In the secondary coil, each single-layer coil winding has different inductance due to the coil configuration. Hence a non-uniform current distribution will occur in the secondary coil at the coil energization. In this study, in order to investigate the characteristics of the secondary coil, the design study of the secondary coil was conducted by modeling the secondary coil with a lumped constant circuit. This paper describes the details and the validity of the model, and the results of the design study under the various conditions of coil windings.

2. Stacked Single-Layer (SSL) Coil Windings

The secondary coil is composed of stacked single-layer (SSL) coils wound with Bi2223 tapes which are insulated with Kapton tapes. Figure 1 (a) illustrates the schematic view of the SSL coil windings, and Fig. 1 (b) shows the electrical circuit of the SSL coil windings. Each single-layer coil winding is connected to current leads composed of HTS tapes with solder at the termination of the single-layer coil windings. All of the current leads are connected to copper plates which are the termination of the secondary coil. Specifications of the secondary coil are listed in Table 1.

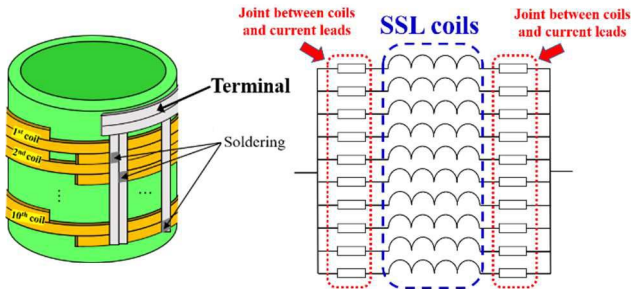

Fig. 1 The schematic view of the secondary coil (a) and the electric circuit of the secondary coil (b).

author's e-mail: obana.tetsuhiro@nifs.ac.jp
*) This article is based on the presentation at the 29th International Toki Conference on Plasma and Fusion Research (ITC29).

Table 1 Specifications of the secondary coil.

Coil diameter	90.3 mm
Height	92.6 mm
Number of coil windings	10
HTS tape width/thickness	4.3 mm / 0.2 mm

3. Modeling

Considering the vertically symmetrical configuration of the secondary coil composed of ten coil windings, a model composed of five coil windings was developed. The circuit equation of the model is given as follows:

$$\sum_{n=1}^{5} L_{m,n}\frac{di_m}{dt} + R_m \cdot i_m = V \qquad (1 \le m \le 5),$$

where i_m is the current at the coil winding m, R_m is the total electrical resistance at the coil winding m, V is the voltage across the coil winding, $L_{m,n}$ is the mutual inductance between the coil winding m and the coil winding n. Provided that the coil winding m is the same position as the coil winding n, $L_{m,n}$ is the self-inductance. The current at the coil winding m is given by

$$\sum_{m=1}^{5} i_m = I_{total},$$

where I_{total} is the total current of the model. The total electrical resistance at the coil winding m is given by

$$R_m = R_{t,m} + R_{sc,m},$$

where $R_{t,m}$ is the joint resistance at terminals of the coil winding m, $R_{sc,m}$ is the electrical resistance of the coil winding m taking into account the superconducting characteristics given by

$$R_{sc,m} = \frac{1}{i_m} \cdot E_c \cdot l \cdot \left(\frac{i_m}{i_{c,m}}\right)^N,$$

where E_c is the critical electrical field which is determined to be 10 μV/m, l is the coil winding length, $i_{c,m}$ is the Ic of the coil winding m, and N is the N value.

4. Validation of the Model

Using the model, the voltage of the secondary coil was calculated during the coil excitation. The Ic and the N value of one coil winding are 160 A and 17, respectively. The magnetic field dependency of Ic and N value is not considered in this model. The joint resistance for each joint between a terminal and coil winding is set as 7.5 μΩ. Figure 2 shows the results of the measurement and the calculation regarding the coil voltages. The coil voltage increases linearly with the increase of the operating current, and then the coil voltage increases sharply after the coil current exceeds approximately 1600 A which is the Ic derived from the specification of the secondary coil. The calculation is in good agreement with the measurement. As a result, the model is considered to be valid for the coil excitation.

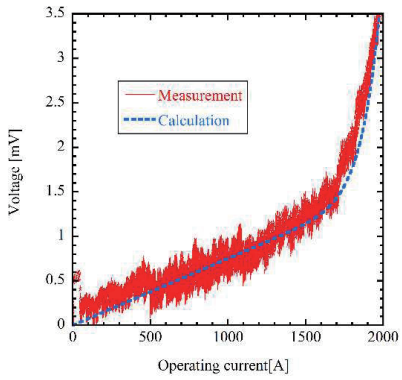

Fig. 2 Comparison between the measurement and the calculation of the secondary coil regarding the coil voltage.

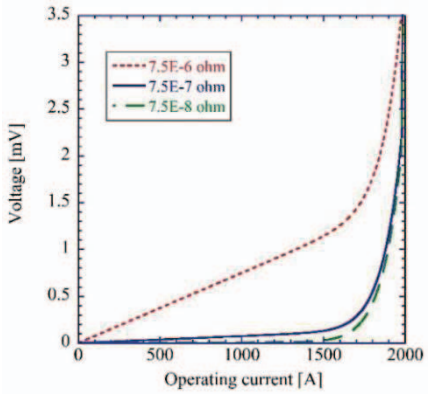

Fig. 3 The voltages of the secondary coil with various joint resistances.

5. Calculation Results and Discussion

5.1 Effect of the joint resistance at terminals on the generated voltage

The secondary coil is composed of HTS coil windings. As shown in Fig. 2, however, the voltage of the secondary coil increases linearly as the operating current of the secondary coil increases when the operating current is lower than the expected Ic of the secondary coil which is 1600 A. As a cause of this phenomenon, joint resistances at the terminals of the secondary coil are considered. Hence, the effect of the joint resistance on the generated voltage of the secondary coil was investigated using the model. In this investigation, the voltage of the secondary coil during the coil excitation was calculated with the different joint resistances (7.5 μΩ, 750 nΩ, and 75 nΩ). Figure 3 shows the calculation results of the coil voltage at each joint resistance. Compared to the voltage at the joint resistance of 7.5 μΩ which was described in Section 4, the voltages at the other resistances are significantly low until the operating current reaches nearly the expected Ic of the secondary coil. Consequently, the joint resistance at the coil winding's terminal must be reduced as much as possible in the coil production to restrain the voltage generated in the SSL

coils.

5.2 Effect of the inductance on the current distribution

The coil windings in the secondary coil have different inductance due to the coil configuration. Hence, there is a concern that a non-uniform current distribution occurs in the secondary coil, which may deteriorate the performance of the secondary coil. To investigate the effect of the inductance on the current distribution, the current distribution of the secondary coil was calculated using the model. In this calculation, the joint resistances at the coil winding's terminal were set as 75 nΩ and 0 Ω, respectively. Figures 4 and 5 show the results of the transport currents in the secondary coil with the joint resistances of 0 Ω and 75 nΩ, respectively. When the joint resistance is 0 Ω, the current distribution depends on the operating current of the secondary coil. The current distribution is non-uniform in the case that the operating current is much lower than the expected Ic of the secondary coil which is 1600 A, and the current distribution is uniform in the case that the operating current is close to or higher than the Ic.

In the case that the joint resistance is 75 nΩ, on the other hand, the current distribution is always uniform.

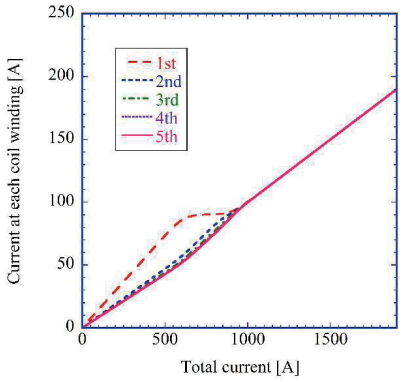

Fig. 4 Transport current at each coil winding with the joint resistance of 0 Ω at coil winding's terminal.

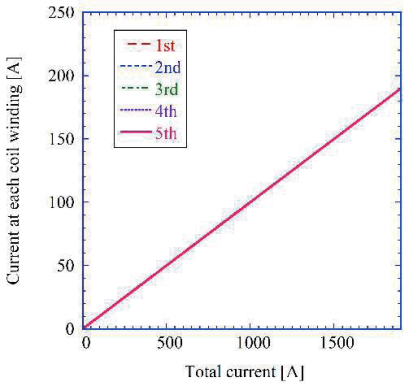

Fig. 5 Transport current at each coil winding with the joint resistance of 75 nΩ at coil winding's terminal.

Consequently, the current distribution of the secondary coil can be uniform due to the joint resistance even though the secondary coil has different inductances in each coil winding.

5.3 Effect of the joint resistance at the coil winding's terminal on the current distribution

As described in Section 5.2, the joint resistance at coil winding's terminal can eliminate the influence of the inductance at each single-layer coil winding, resulting in making the current distribution of the secondary coil uniform. Note that the joint resistance was made uniform at each single-layer coil winding in the model used in Section 5.2. In this section, the influence of the joint resistance at coil winding's terminal on the current distribution of the secondary coil was investigated. The model with different joint resistances for each single-layer coil was used in this study. Table 2 shows the joint resistances for each coil winding using the model. The calculation result of the current distribution in the secondary coil is shown in Fig. 6. In the case that the total current of the secondary coil is lower than the expected Ic of the secondary coil which is 1600 A, the single-layer coil winding with a lower joint resistance has a larger coil current. Hence, the joint resistance has an effect on the current distribution of the secondary coil.

On the other hand, in the case that the total current of the secondary coil is larger than the Ic, the transport current becomes uniform at each single-larger coil winding. Under this condition, there is no influence of the joint resistance on the current distribution of the secondary coil. Considering the operation of the secondary coil, each joint resistance at the terminal should be uniform in the coil production.

Table 2 Joint resistance at each coil winding.

	1st	2nd	3rd	4th	5th
R [nΩ]	75	80	85	90	95

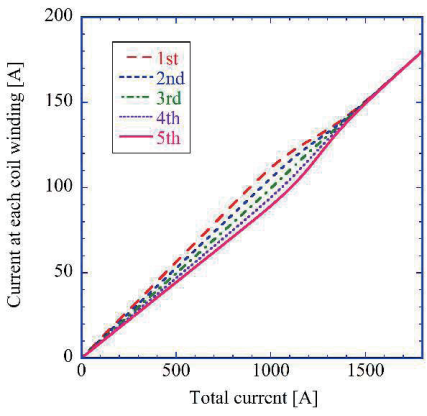

Fig. 6 Transport current at each coil winding with different joint resistances.

5.4 Effect of the tape's Ic degradation on the coil performance

HTS tapes are sensitive for mechanical stress, such that there is a concern that the performance of the tapes is degraded due to coil winding work. In this section, the effect of the tape's degradation on the secondary coil's performance was investigated for the purpose of obtaining reference data for coil development. The model considering the coil wound with degraded HTS tapes was used in the simulation. Regarding the model composed of five single-layer coils which are described in Section 3, the Ic and the N value of the first single-layer coil were changed at each condition. On the other hand, the Ic and the N value of the other single-layer coils were set as 160 A and 17, respectively. For each coil winding, the joint resistance at the coil winding's terminal was set as 75 nΩ. The current distribution and the voltage of the secondary coil during the coil excitation were calculated using the model. Figures 7 (a), (b), and (c) show the calculation results of the secondary coil under the various conditions of the first single-layer coil. Regarding the voltage in the secondary coil, the lower the performance of the first single-layer coil, the easier the coil voltage will occur during the coil excitation.

The current distribution in the secondary coil is also influenced by the degraded performance of the first single-layer coil. As the performance of the first single-layer coil decreases, the current distribution in the secondary coil becomes more uneven. Note that when the total current increases, the current in the first single-layer coil suddenly drops compared to the current in the other single-layer coils. However, as the coil voltage increases, the current in the first single-layer coil sharply increases, and the uneven current distribution in the secondary coil is slightly improved.

6. Conclusion

The secondary coil composed of the SSL coils was modeled with a lumped constant circuit. Using the model, the voltage of the secondary coil was calculated during the coil excitation. The calculation was in good agreement with the measurement. The result indicates that the model is valid for the coil excitation. The effect of the joint resistance at the coil terminals on the characteristics of the secondary coil was investigated. As a result, the current distribution of the coil can be uniform due to the joint resistance even though the coil has different inductance in each coil winding. Moreover, the effect of the HTS tape's degradation on the secondary coil's performance was investigated. Consequently, the current distribution and the voltage of the secondary coil are influenced by the tape's degradation.

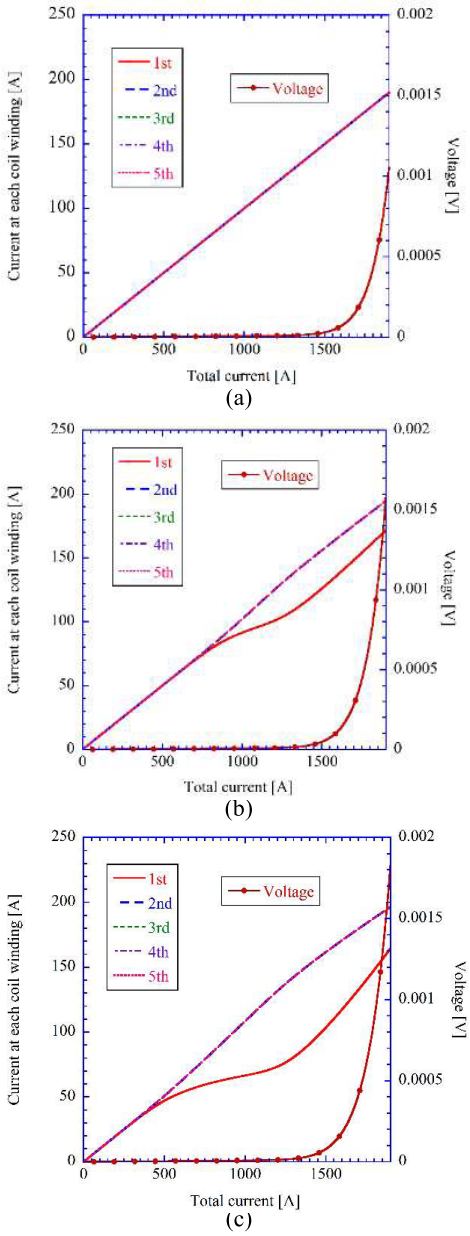

Fig. 7 The voltage of the secondary coil and the transport current at each coil winding (a) in the case that Ic is 160 A and N value is 17 for the 1st coil winding, (b) in the case that Ic is 130 A and N value is 12 for the 1st coil winding, and (c) in the case that Ic is 100 A and N value is 7 for the first coil winding.

Acknowledgments

This work was supported by the NIFS Collaborative Research Program (NIFS19KECA072).

[1] N. Nanato *et al.*, J. Phys. Conf. Series **1054**, 012070 (2018).
[2] N. Nanato *et al.*, J. Phys. Conf. Series **1293**, 012072 (2019).